Flow Resistance and Design Guidelines for Embankment Stepped Chutes

C.A. Gonzalez
Water Engineering section, Cardno Pty. Ltd, 5 Gardner Close, 4064, QLD. Australia

H. Chanson
Department of Civil Engineering, The University of Queensland, 4072, QLD. Australia

Abstract: Recently the design flows of many dams have been re-evaluated, resulting in spills often larger than the original ones. In many cases, occurrence of revised flows would result in dam overtopping because of insufficient storage and spillway capacity of reservoirs. Embankment dams whilst common are more likely to fail than other dam types when overtopped in an uncontrolled manner because of breaching or complete erosion of the downstream face of the embankment. Despite the catastrophic effects of dam failure, dam overtopping constitutes still most identified collapses. Stepped chutes with moderate slopes represent a convenient embankment overtopping protection because of its large energy dissipation potential and its compatibility with recent construction methods (RCC, rip-rap gabions). New experimental flow resistance results are presented herein to help designers to predict accurately energy dissipation on moderate slope stepped chutes. Some recent advances in design guidelines are also discussed.

Keywords: stepped chutes, flow resistance, embankment protection

1 INTRODUCTION

Before the 1980's, overtopping counter-measures consisted mainly of increasing either reservoir storage or spillway capacity. Lately overtopping protection systems have gained acceptance because they safely allow controlled flows over the dam wall during large flood events (Figure 1).

Figure 1. Melton dam secondary spillway (Australia, 1916)

There are several techniques to armour embankment slopes, including paving, rip-rap gabions, reinforced earth, pre-cast concrete slabs and roller compacted concrete (RCC). With RCC and gabions, placement techniques yield embankment protections shaped in a stepped fashion. The introduction of such new construction techniques and materials have also led to the development of new applications for stepped chutes (e.g. re-aeration cascades, fish ladders and stepped channels for river training) allowing cheaper construction and increased interest in staircase channels.

Despite these recent interests, the characteristics and performances of stepped chutes flows with moderate slopes are not yet totally understood mainly because most earlier studies were focused on flows down steep chutes ($\theta \sim 45^{o}$). Up to date, no analytical model is able to predict the properties of the highly turbulent two-phase stepped chute flow.

This study details an experimental investigation of the hydraulic performances of moderate-slope stepped chutes. It aims to understand the turbulent air-water flow energy dissipative processes occurring down stepped chutes. It also provides new, original insights into air-water stepped spillway flows not foreseen in prior studies and it presents a new design criterion for stepped chutes with moderate slopes typical of embankment dams.

2 EXPERIMENTAL SETUP

This study involved large, near full-scale physical modeling of stepped spillway flow with moderate slopes based upon a Froude similitude.

Measurements were conducted at the University of Queensland in two large physical models: a 3.15 m long, 15.9° slope stepped chute with two interchangeable step heights (h = 0.1 m and h = 0.05 m) and a 2.5 m long, 21.8° slope stepped channel with 0.1 m step height. A broad range of discharges within transition and skimming flow regimes was investigated (Table 1).

The size of the models (h = 0.1 m and 0.05 m, W = 1 m) corresponded to a geometric scaling ratio of about L_r = 3 to 6 for a typical prototype step height h = 0.3 m that is a common geometry for RCC and gabion overflow embankment spillways. The large size of the experiments ensured the extrapolation of model results to prototype with minimum scale effects. Boes (2000), Chanson et al. (2002) and Gonzalez and Chanson (2004a) discussed scale effects in air-water stepped chute flows and emphasized the need for large-size models.

Table 1 Experimental flow conditions

Channel	θ^o	q_w (m²/s)	h (m)	d_c/h	Flow regime	Remarks
Channel 1						
	16	0.075 to 0.22	0.1	0.6 to 1.5	transition and skimming	L =3.3m W = 1m
	16	0.02 to 0.2	0.05	0.7 to 3.2	transition and skimming	L =3.3m W = 1m
Channel 2						
	22	0.1 to 0.18	0.1	1.1 to 1.5	skimming	L =3.3m W = 1m

Note: L : chute length; W: chute width; θ : chute slope ; h: step height; d_c : critical depth at crest ; q_w: discharge per unit width.

Experiments included detailed air-water flow properties measurements obtained using a double tip conductivity probe (Ø = 0.025 mm). The probe output signals were scanned at 20 kHz for 20 s per sensor (Toombes 2002(2002), Gonzalez 2005). The probe translation in the direction normal to the flow was conducted using a digital ruler within 0.1 mm.

Measurements were conducted with the double-tip probe located on the channel centreline at and between each step edge. In the direction normal to the flow, measurements were conducted from y = 0 up to the spray region. In the flow direction, measurements were performed at step edges and in between at dimensionless distances X_0 = 0.25, 0.5 and 0.75 where $X_0 = x/L_{cav}$, x is the distance from the upper step edge to the probe-tip and L_{cav} is the distance between step edges.

2.1 Data processing

The probe consisted of two tips, aligned in the flow direction that detect the difference in conductivity between air and water and record the number of air bubbles striking both tips sequentially (Fig. 2). The resulting voltage signals allowed measurement of air concentration, bubble count rate, air-water flow velocity and turbulence intensity.

The air concentration C is the proportion of time that the leading tip is in air and the bubble count rate F is the number of bubbles impacting the probe tip. Velocity measurements were based upon the time delay for bubbles successively striking both leading and trailing tips. A cross-correlation technique was used to calculate velocity (Crowe et al., 1998).

$$V = \frac{\Delta x}{T} \tag{1}$$

where Δx is the distance between tips and T is the time for which the cross-correlation R_{xy} is maximum (Fig. 2).
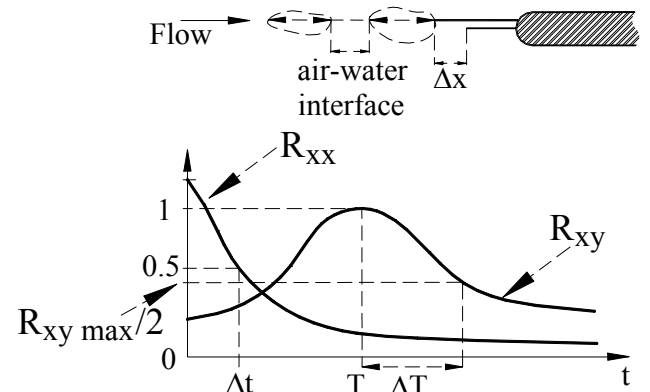

Figure 2. Air-water flow velocity and turbulence intensity measurement technique

The turbulence intensity was deduced from the standard deviation of the velocity as:

$$Tu = 0.851 \cdot \sqrt{\frac{\Delta T^2 - \Delta t^2}{T}} \tag{2}$$

where ΔT is a time scale corresponding to half of the maximum value of the normalized cross-correlation function R_{xy} and Δt is a time scale for which the normalized autocorrelation function R_{xx} equals 0.5 (Fig. 2).

3 BASIC AIR WATER FLOW RESULTS

Flow over a stepped cascade is divided into three separate flow regimes depending on the flow rate for

a given stepped chute geometry: nappe, transition and skimming flow regimes with increasing flow rate. In this study, transition and skimming flows were investigated although the main focus was on skimming flows.

Transition flows were observed for the lowest range of investigated discharges. Strong hydrodynamic fluctuations, splashing and spray near the free surface were the main features of this flow regime. Different sized air cavities alternating with fluid-filled recirculation vortices were observed between step edges below the mainstream of the flow. To date transition flow properties cannot be predicted accurately as very little information is available

Skimming flow was observed for larger discharges. In skimming flow regime the water skims over the pseudo-bottom formed by the step edges as a coherent stream. Beneath the pseudo-bottom intense recirculation vortices fill the cavities between all step edges (Chamani and Rajaratnam 1999). These recirculation eddies are maintained by the transmission of shear stress from the mainstream and contribute significantly to the energy dissipation. Visual inspections highlighted their three-dimensional nature. Three to four spanwise recirculation cells were observed across the channel width. The findings were consistent with observations by Matos and Yasuda (Pers.comm.) on steeper chutes. The vortices are related to streamwise coherent structures in the mainstream.

Skimming flows exhibit an appearance similar to flows down a smooth chute. The upstream end has a smooth and transparent look characteristic of clear-water flow. However next to the upstream inlet of the chute a boundary layer develops. When the outer edge of this boundary layer reaches the free surface, the turbulence induces natural aeration giving the flow its white, foamy appearance. This point is called the point of inception of air entrainment. Immediately downstream the point of inception, rapid flow aeration is observed and the flow varies gradually until it becomes fully developed, further downstream the flow reaches equilibrium and its properties do not vary with longitudinal distance.

For stepped chutes with flat to moderate slopes, Chanson (2002) and Ohtsu et al. (2004) proposed a further subdivision of skimming flows: subregime SK1 for the lowest range of discharges and a subregime SK2 for the upper range. In SK1, a wake forms downstream of each step edge with a recirculating vortex underneath. The wake and the vortex do not extend over the full step length and the

water impacts in the horizontal part of the step. Skin friction drag occurs on the step. The water surface is parallel to the horizontal part of the steps. For SK2, the wake and the recirculating eddy region extend the full length of the step sometimes interfering with the developing wake of the subsequent step, preventing skin friction drag on the step to occur. The water surface is parallel to the pseudo-bottom formed by the step edges most of the time. In this study, a SK1 flow regime was observed for all investigated conditions in both channels.

Figure 3 summarises criterions provided by Chanson (2002) and Ohtsu et al. (2004) to predict changes in flow regimes on stepped chutes depending on discharge and step geometry. They are based on large-size experiments.
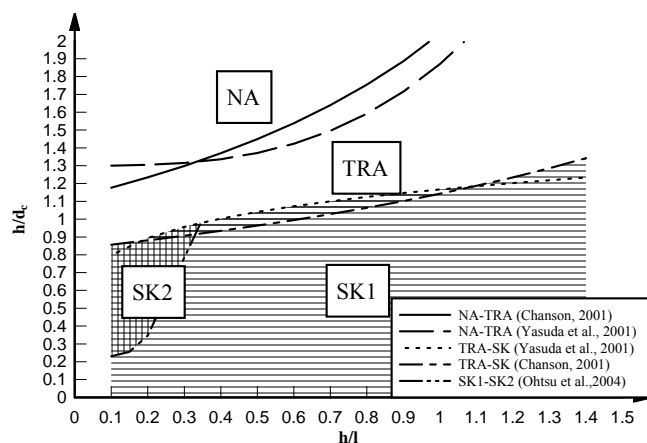
Figure 3. Prediction of flow regime on stepped chutes

3.1 Air concentration and velocity

Detailed measurements of air-water flow properties were conducted downstream of the point of inception of air entrainment. Figure 4 presents typical air concentration distributions obtained at and in between step edges in both channels, where Y_{90} is the characteristic flow depth at $C = 0.9$ and V_{90} the corresponding velocity. The symbol description is given in Table 2.
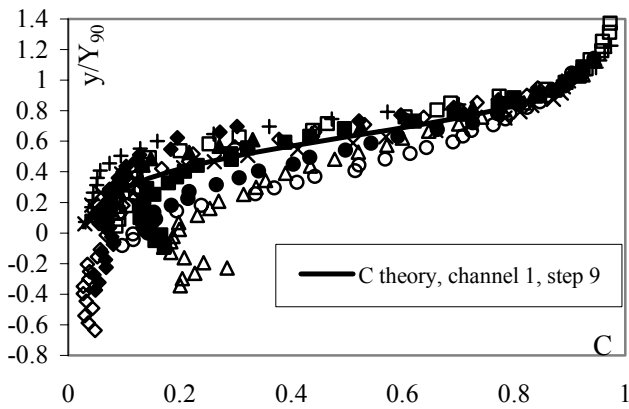
Figure 4. Experimental air concentration distributions

Table 2. Symbols for Figures 4 to 7

$\theta = 16^o$, h = 0.1		$\theta = 16$, h = 0.05		$\theta = 22^o$, h = 0.1	
□	step 8	+	step 10	▲	step 9
◇	81	×	step 11	◆	91
△	82			■	92
○	83			●	93

Note: 81, 82 and 83 denote positions X_0 = 0.25, 0.5 and 0.75 in between step edges 8 & 9 respectively. 91, 92 and 93 denote similar positions between step edges 9 & 10.

It can be observed that void fraction data obtained above the pseudo-bottom (y > 0) were similar for all configurations and followed closely an analytical solution of the advective diffusion equation (Chanson 1995,2002). Data obtained at the downstream end of cavities suggested a greater overall aeration of the cavity flow (y < 0) between step edges. Matos et al. (2001) reported a similar finding. Additionally, the comparison of data for two different step sizes (channel 1) demonstrated that air concentration distributions were properly scaled with a Froude similitude.

Chanson and Toombes (2002) hypothesized that inertia forces acting on air bubbles trapped in the core of the recirculating vortices enhanced cavity aeration and led to higher air content in between step edges. Present results support such a hypothesis.

Figure 5 presents typical air-water velocity data collected at and in between step edges in both chutes operating with skimming flows. Data profiles obtained at step edges followed closely a power law:

$$\frac{V}{V_{90}} = \left(\frac{y}{Y_{90}}\right)^{\frac{1}{n}} \quad for \quad \frac{y}{Y_{90}} \leq 1 \quad and \quad \frac{V}{V_{90}} = 1 \quad for \quad \frac{y}{Y_{90}} \geq 1 \quad (3)$$

where V_{90} is the characteristic velocity at $y = Y_{90}$.

For skimming flows (1.1 < d_c/h < 1.5) the values of the exponent "n" oscillated between 7.8 and 11.8.
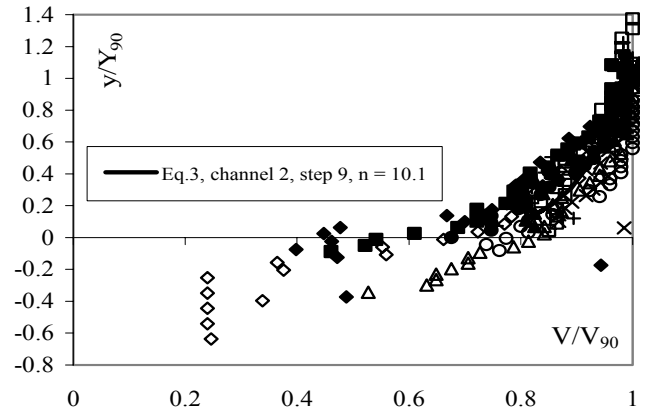

Figure 5. Experimental air-water flow velocity distributions

Measurements between step edges exhibited significant differences particularly for $y/Y_{90} \leq 0.3$, suggesting greater flow velocities immediately above the recirculation zone. Results highlighted the effects of the developing shear layer downstream of each step edge on the air-water flow, both in the recirculating cavity region and the mainstream flow (Gonzalez and Chanson, 2004a). Good agreement was also observed with data obtained using a smaller step size ($\theta = 16^o$, h = 0.05 m) demonstrating that velocity distributions were properly scaled with a Froude similitude (Chanson and Gonzalez, 2005).

3.2 *Turbulence intensity and bubble count rate*

Air-water flow turbulence intensity (Tu) profiles for both channels are presented in Figure 6. The data indicated very high turbulence levels, with maximum values above 100 %. These values were consistent with turbulence intensities in wake flows between rocks obtained by Sumer et al. (2001) and in the clear water zone of skimming flows by Ohtsu and Yasuda (1997) and Amador et al. (2004). The data suggested higher turbulence in stepped chute skimming flows than in smooth chute clear-water flows.
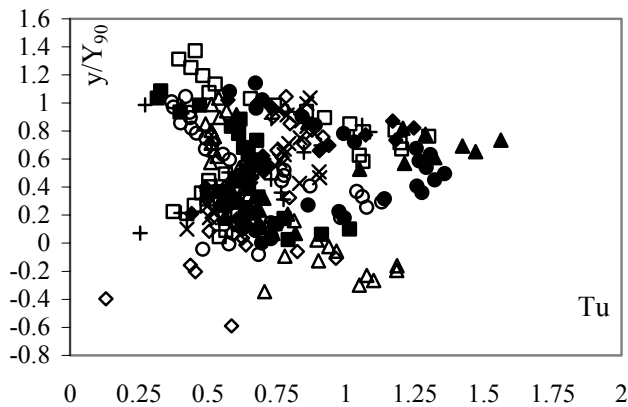
Figure 6. Air-water flow turbulence intensity distributions

Figure 7. Experimental bubble countrate distributions

Turbulence data collected between step edges also suggested an increase in turbulence towards the downstream end of the cavity ($X_0 \geq 0.5$). For example, in Figure 6, maximum turbulence levels Tu_{max} were about 80, 110 and 140 % for $X_0 = 0.25$, 0.5 and 0.75 respectively. The findings were consistent with visual observations of cavity fluid ejection and replenishment, taking place primarily in the downstream half of the cavity. At the upstream half of the cavity ($X_0 < 0.5$) turbulence data showed significantly different trends to data obtained in the downstream half. The influence of the developing shear layer and the transfer of momentum between mainstream and cavity recirculation were believed to cause the differences.

Chanson and Toombes (2002) hypothesized that the high turbulence levels were directly linked to the number of entrained bubbles/droplets and may be attributed to a number of factors, including particle collisions, break-up and coalescence affecting the interfacial velocity field. It is also believed that high flow resistance associated with form drag generated by the steps, contributed to strong turbulent mixing throughout the entire flow yielding to high turbulence intensity levels (Gonzalez, 2005).

In Channel 1 ($\theta = 16°$), differences in turbulence intensities were consistently observed between h = 0.05 & 0.10 m, with lesser maximum turbulences for the smallest step height (h = 0.05 m). This is illustrated in Figure 6 and highlight some scale effects in terms of turbulence intensity with a Froude similitude (Gonzalez and Chanson, 2004b)
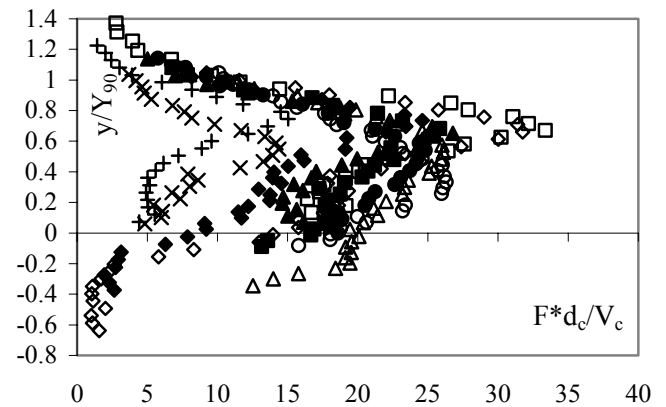
Dimensionless bubble frequency $F*d_c/V_c$ distributions are presented in Figure 7 where F is the bubble count rate and d_c and V_c are the critical flow depth and velocity respectively.

Bubble count rate data were similar for both chutes with large step sizes (h = 0.1 m). However significant differences were observed in terms of bubble count rate distributions. In channel 1, lesser bubble count rates (by about 30 to 50%) were observed for the smallest step height (h = 0.05 m). This is illustrated in Figure 7. The findings imply significant scale effects in terms of number of entrained bubbles and bubble sizes.

3.3 Energy dissipation

In smooth channel energy dissipation occurs predominantly through friction loss. On stepped cascades, additional energy dissipation mechanisms exist, including cavity recirculation vortices beneath the mainstream, momentum exchange between the main flow stream and the mixing layer formed downstream of each step edge and skin friction at the downstream half of the steps. These mechanisms cause significant form drag in stepped spillways.

Despite their limitations, Darcy-Weisbach formulas were utilized in this study to estimate the form losses in the stepped channel because they are still widely used for open channel design. For uniform equilibrium flow in a wide channel, the boundary friction counteracts the gravity force component in the flow direction and the flow depth and velocity may be determined from the momentum principle

$$\tau_0 \cdot P_w = \rho_w \cdot g \cdot A_w \cdot \sin\theta \qquad (4)$$

where τ_0 is the average shear stress between the skimming flow and recirculating fluid underneath,

P_w is the wetted perimeter, A_w the water flow cross-section area and θ is the mean bed inclination angle. In dimensionless terms, and for a wide channel with free-surface flow aeration, Equation 4 becomes:

$$f_e = \frac{8\tau_0}{\rho_w \cdot U_w^2} = \frac{8 \cdot g}{q_w^2} \cdot \left(\int_{y=0}^{y=Y_{90}} (1-C)dy \right)^3 \cdot \sin\theta \qquad (5)$$

where f_e is the equivalent Darcy friction factor for air water flow, C the local void fraction, y is the flow depth measured normal to the pseudo-invert, U_w is the mean flow velocity with $U_w = q_w/d$, q_w is the water discharge per unit width, C_{mean} is the mean air concentration and d is the equivalent clear water depth:

$$d = (1 - C_{mean}) \cdot Y_{90} \qquad (6)$$

In gradually varied skimming flows, the average shear stress between the mainstream and the cavity recirculation must be deduced from the friction slope. For a wide channel, the energy equation yields:

$$f_e = \frac{8 \cdot g}{q_w^2} \cdot \left(\int_{y=0}^{y=Y_{90}} (1-C)dy \right)^3 \cdot S_f \qquad (7)$$

where g is the gravity acceleration, and S_f is the friction slope. Since both channels utilized in this study were relatively short, the flow did not reach uniform equilibrium status at the downstream end and flow resistance estimates were based upon Equation 7.

Equivalent Darcy friction factors based upon data collected at step edges are presented in Figure 8. Results comprise data obtained in both channels, as well as experimental data collected by Chanson and Toombes (2001) in the same facilities, and experimental data obtained in 11.3° and 19° slope stepped channels (h = 0.025, 0.0393, 0.05 & 0.0785 m) by Yasuda and Ohtsu (1999). Results are also compared with a rough, non-physical fit corresponding to 188 experimental data obtained in flat slope laboratory models (Chanson et al., 2002):

$$\frac{1}{\sqrt{f_m}} = 2.43 - 0.2676 \cdot \ln\left(\frac{h \cdot \cos\theta}{D_H} \right) \qquad (8)$$

where f_m is a friction factor obtained from laboratory data with flat slopes and D_H the hydraulic diameter.
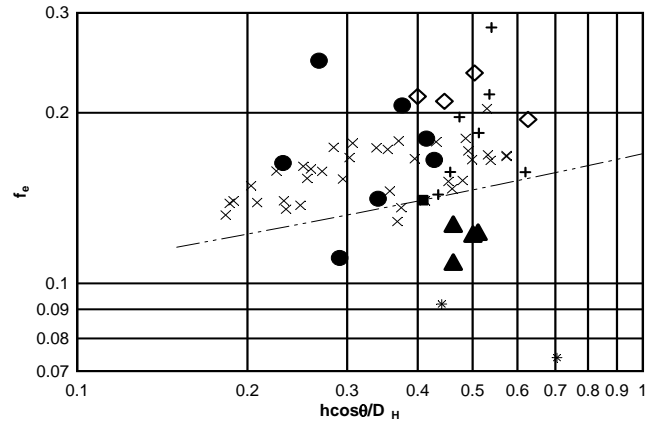

Figure 8. Friction factors for skimming flows in moderate slope stepped chutes

Table 3. Symbology for Figure 8

Chute geometry		Reference
$\theta = 16^o$, h = 0.1 m	▲	(Gonzalez 2005)
$\theta = 16^o$, h = 0.05 m	●	(Gonzalez 2005)
$\theta = 16^o$, h = 0.1 m	■	(Chanson and Toombes 2001)
$\theta = 22^o$, h = 0.1 m	◇	(Gonzalez 2005)
$\theta = 22^o$, h = 0.1 m	⊙	(Chanson and Toombes 2001)
$\theta = 22^o$, h = 0.1 m	▤	(Chanson and Toombes 2001)
$\theta = 22^o$, h = 0.1 m	◆	Yasuda and Ohtsu (1999)
Eq. 4 for $\theta = 16^o$, h = 0.1 m.	▬ ▬ ·	

Overall, the friction factor data for skimming flows were consistent with the re-analysis of Chanson et al. (2002). For the largest step height in channel 1 ($\theta = 16^o$, h = 0.1 m), present data averaged $f_e = 0.12$ while, for channel 2 ($\theta = 22^o$, h = 0.1 m), the data averaged $f_e = 0.19$ suggesting that flow resistance increased slightly with channel slope, within the range of moderate slopes as previously proposed by Ohtsu and Yasuda (1997).

For the smaller step height in channel 1 ($\theta = 16^o$, h = 0.05 m), the average flow resistance was $f_e = 0.18$. The finding suggests that, although the geometrically similar models were scaled with a ratio of only $L_r = 2$, the flow resistance was larger for the smallest step height (h = 0.05 m). It must be noted that this conclusion is based upon a limited data set but illustrates potential scale effects.

4 DESIGN CRITERION

Despite the increasing popularity of moderate slope stepped chutes, most studies and design criterions are limited to steep chutes ($\theta \approx 30$ to 50°). Only two design criterions referred to the hydraulic performance of stepped cascades with flat to

moderate slopes ($11^\circ < \theta < 30^\circ$; Chanson 2002, Ohtsu et al. 2004). Despite these studies, there are still a number of key issues not completely understood in stepped chute flows. Thus, design criterions need to be improved, specifically in terms of flow resistance.

The present criterion can be used for moderate slope chutes ($11^\circ < \theta < 22^\circ$) with skimming flows at design conditions ($1.1 < d_c/h < 1.5$).

Skimming flow is recommended to pass large water discharges while nappe flow is best to achieve maximum energy dissipation rate. Transition flows should be avoided as they might produce dangerous dynamic loads to the structure. It is important that the designer not only account for the design flow rate but also smaller flow conditions.

When designing a stepped spillway, the dam height, the downstream slope of the dam and the design water discharge are generally given. Parameters to be chosen are the type of flow and the step height. However, the designer is often limited to select a step height (h) within the values determined by the dam construction technique (h = 0.2 to 0.9 m with RCC or gabions).

The first step is then to calculate the critical depth at the crest.

$$d_c = \sqrt[3]{\frac{Q_w^2}{g \cdot W^2}} \tag{8}$$

Secondly, the step height should be selected to ensure that the chute will operate with skimming flow conditions (Fig. 3).

The position of the point of inception should be located to ensure that free-surface flow aeration occurs in the upstream end of the chute to achieve uniform equilibrium flow conditions before the toe of the chute. Its coordinates might be calculated as:

$$\frac{L_I}{h\cos\theta} = 9.719\sin\theta^{0.0796}\left(\frac{q_w}{\sqrt{g\sin\theta\left(h\cos\theta\right)^3}}\right)^{0.713} \tag{9}$$

$$\frac{d_I}{h\cos\theta} = \frac{0.4034}{\left(\sin\theta\right)^{0.04}}\left(\frac{q_w}{\sqrt{g\sin\theta\left(h\cos\theta\right)^3}}\right)^{0.592} \tag{10}$$

where L_I and d_I are the length to and depth at the inception point (Chanson 1995).

Designers must also consider a maximum value of d_c/h above which the steps become too small and no longer act as a large roughness. Chanson (1995) suggested a maximum step height limit of:

$$h \le 15 \cdot d_c \cdot \cos\theta \tag{11}$$

Further, fully developed condition must preferably be achieved before the toe of the stepped chute. However this is not always possible.

$$\frac{d_c}{h} < \frac{1}{0.1193 \cdot \cos\theta \times \sin\theta^{0.259} \times \left(\dfrac{L}{h \cdot \cos\theta}\right)^{0.935}} \tag{12}$$

After this point, designers should follow different paths depending if uniform equilibrium flow conditions are achieved or not.

If the channel is long enough for the flow to reach uniform equilibrium conditions, the characteristic flow depth d should be calculated as:

$$d = d_c \cdot \sqrt[3]{\frac{f_e}{8 \cdot \sin\theta}} \tag{13}$$

where f_e is the Darcy friction factor estimated based upon experimental air-water flow friction factor data as suggested by Chanson (2002).

In air-water flows, friction factors f_e decrease with increasing mean air concentration C_{mean}, hence f_e should be calculated as:

$$\frac{f_e}{f_m} = 0.5 \cdot \left(1 + \tanh\left(2.5 \cdot \frac{0.5 - C_{mean}}{C_{mean} \cdot (1 - C_{mean})}\right)\right) \tag{14}$$

where f_m should be deduced with Equation 8 and the average C_{mean} might be computed based upon a criterion developed by Ohtsu et al. (2004):

$$C_{mean} = D - 0.3 \cdot e^{\left\{-5 \cdot \left(\frac{h}{d_c}\right)^2 - 4 \cdot \left(\frac{h}{d_c}\right)\right\}} \tag{15}$$

where D = 0.3 for $5.7^\circ < \theta < 19^\circ$, D = $-0.00024\theta^2 + 0.0214\theta - 0.0357$ for $\theta \ge 19^\circ$

Finally, based on the obtained depth, the velocity ($U_w = q_w/d$), Y_{90} (Equation 6) and the height of the sidewalls h_w should be estimated ($h_w = 1.4 \cdot Y_{90}$).

If the flow does not reach uniform equilibrium flow conditions before the toe of the chute, the air-water flow depth should be deduced from the integration of the backwater equation.

$$S_f = -\frac{\partial H}{\partial x} = \sqrt{\frac{f_e}{8}} \cdot \frac{q_w^2}{g \cdot d^3} \tag{16}$$

Several researchers have attempted to use the backwater equation to calculate water depth and Darcy friction factors making gross assumptions violating basic principles as it is only valid for fully-developed flows (Chanson, 2002). This method is tedious and may not be suitable for all cases.

Alternatively the flow properties in the gradually varied flow region can be calculated with a smooth correlation curve obtained by linking best documented experimental results at the developing and the equilibrium flow regions (Gonzalez, 2005)

$$\frac{U_w}{V_{max}} = 0.00107 \cdot \left(\frac{H_{max}}{d_c}\right)^2 - 0.0634 \cdot \left(\frac{H_{max}}{d_c}\right) + 1.202 \qquad (17)$$

where H_{max} is the upstream total head, d_c is the critical depth and V_{max} is the ideal flow velocity. Once the dimensionless downstream velocity is known, the flow properties can be estimated assuming fully developed flow conditions. The friction factor in skimming flow is typically $f_e = 0.2$. Finally, the ideal fluid flow velocity is can be estimated from the Bernoulli equation:

$$V_{max} = \sqrt{2 \cdot g \cdot H_{max} - (d \cdot \cos\theta)} \qquad (18)$$

Once, the velocity and depth of the flow are obtained, the average air concentration C_{mean}, Y_{90}, (Eq. (6) and (8)) and the height of the sidewalls h_w can be computed ($h_w = 1.4 \cdot Y_{90}$).

This alternate method may be used for preliminary design calculations, however it is important to note that it was obtained assuming $f_e = 0.2$ as in the uniform equilibrium region and it was only validated for skimming flow in stepped chutes with moderate slopes ($16^o < \theta < 22^o$).

Designers should be aware that embankment overflow stepped spillway design is a critical process, as any failure can lead to a catastrophe. A number of key parameters should be assessed properly, including stepped face erosion, seepage through the embankment, drainage beneath the steps, interactions between the abutments and the stepped face, etc. (Gonzalez and Chanson, 2004c). In turn, physical modeling with scaling ratios no greater than 3:1 is strongly advised.

5 CONCLUSION

Flow cascading down a staircase channel with moderate slopes has been little studied and physical properties are not totally understood. The strong aeration and high turbulence of the flow prevented the use of analytical models to predict flow properties. An experimental study was conducted herein based on Froude similitude in large-size experimental facilities to gain a better understanding of the flow properties in stepped chutes with slopes typical of embankment dams. Results included air water flow properties such as air concentration, flow velocity, turbulence, and bubble count rate. Based on measured velocities, the flow resistance was estimated accurately. Equivalent Darcy-Weisbach friction factors for moderate slope stepped chutes were larger than those for smooth chutes averaging a value of $f_e = 0.19$. In addition some scale effects were observed in terms of bubble count rate, turbulence intensity and flow resistance. Based on present results, a new design criterion was proposed. Although is based on limited experimental data, the criterion assessed key issues not foreseen in prior studies (gradually varied flow, type of flow regime and flow resistance). While the findings were obtained for two moderate slopes ($\theta = 16$ & 22°), it is believed that the outcomes are valid for a wider range of chute geometry and flow conditions.

BIBLIOGRAPHY

Amador , A., Sanchez-Juny, M., Dolz, J., Sanchez-Tembleque, F., and Puertas, J.(2004). "Velocity and pressure measurements in skimming flows in stepped spillways." Intl. conf. on hydraulics of dams and river structures, Teheran, Iran.

Boes, R.(2000). "Scale effects in modelling two-phase stepped spillway flows." Intl. workshop on hydraulics of stepped spillways, Zurich, Switzerland, 163-170.

Chanson, H. (1995). Hydraulic Design of Stepped cascades, Channels, Weirs and Spillways, Pergamon, Oxford.

Chanson, H., and Gonzalez, C. A. (2005). "Physical modelling and scale effects of air-water flows

on stepped spillways." Journal of Zhejiang University SCIENCE, 6A(3), 243-250.

Chanson, H., and Toombes, L. (2001). "Experimental Investigations of Air Entrainment in Transition and Skimming Flows down a Stepped Chute: Application to Embankment Overflow Stepped Spillways." Research report; no. CE158, Dept. of Civil Engineering, University of Queensland, Brisbane, Australia.

Chanson, H., and Toombes, L. (2002). "Air-water Flows Down Stepped Chutes: Turbulence and Flow Structure Observations." Intl. Journal of Multiphase Flow, 28(11), 1737-1761.

Chanson, H., Yasuda, Y., and Ohtsu, I. (2002). "Flow Resistance in Skimming Flows in Stepped Spillways and its Modelling." Canadian Journal of Civil Engineering, 29(6), 809-819.

Crowe, C. T., Sommerfeld, M., and Tsuji, Y. (1998). Multiphase Flows with Droplets and Particles, CRC Press, Boca Raton, USA.

Gonzalez, C. A. (2005). "An experimental study of free-surface aeration on embankment stepped chutes," Thesis (Ph.D.) - University of Queensland, 2005., [St. Lucia, Qld.],.

Gonzalez, C. A., and Chanson, H. (2004a). "Interactions between Cavity Flow and Mainstream Skimming Flows: An Experimental Study." Canadian Journal of Civil Engineering, 31(1), 33-44.

Gonzalez, C. A., and Chanson, H.(2004b). "Scale Effects in Moderate Slope Stepped Spillways
Experimental Studies in Air-Water Flows." 8th National Conference on Hydraulics in Water Engineering, Gold coast, Australia.

Gonzalez, C. A., and Chanson, H.(2004c). "Stepped spillways for embankment dams: Review, progress and developments in overflow hydraulics." Intl. conf. on hydraulics of dams and river structures, Teheran, Iran, 287-294.

Matos, J. (2001). "Onset of Skimming Flow on Stepped Spillways - Discussion." Journal of Hydraulic Engineering-Asce, 127(6), 519-521.

Ohtsu, I., and Yasuda, Y.(1997). "Characteristics of Flow Conditions on Stepped Channels." IAHR Biennial Congress, San Francisco, USA.

Ohtsu, I., Yasuda, Y., and Takahashi, M. (2004). "Flow Characteristics of Skimming Flows in Stepped Channels." Journal of Hydraulic Engineering-ASCE, 130(9), 860-869.

Sumer, B. M., Chua, L. H. C., Cheng, N. S., and FredsØe, J. (2001). "Suction Removal of Sediment from between Armor Blocks." Journal of Hydraulic Engineering-Asce, 127(4), 293-306.

Toombes, L. (2002). "Experimental Study of Air-water Flow Properties on Low-gradient Stepped Cascades," Ph.D, The University of Queensland, Brisbane.

Yasuda, Y., and Ohtsu, I.(1999). "Flow Resistance of Skimming Flow in Stepped Channels." Proc. 28th IAHR Congress, Graz, Austria.